Letters

Characterization of gel-grown single crystals of strontium tartrate tetrahydrate

Single crystal growth of SrTr (strontium tartrate tetrahydrate, $SrC_4H_4O_6 \cdot 4H_2O$) in silica gels has been reported in the literature [1, 2]. The latter report [2] pertains to the growth of one of the largest (two inches across) gel-grown product. The present paper aims to describe the observations made on the growth mechanism, imperfections, selective etching behaviour and some physical properties of these crystals.

With a view to gaining information regarding the mechanism and history of crystal growth, the habit faces were examined under an optical microscope. The {1 0 1} faces of macrodome and brachypinacoid habit showed flat and smooth surfaces, while the {0 1 0} faces exhibited features such as shown in Fig. 1, in which piling and spreading up of growth layers is quite apparent. Supported by Strickland-Constable [3], and in the absence of growth spirals and hillocks, a two dimensional layer growth mechanism is believed to be operative for the growth of SrTr crystals.

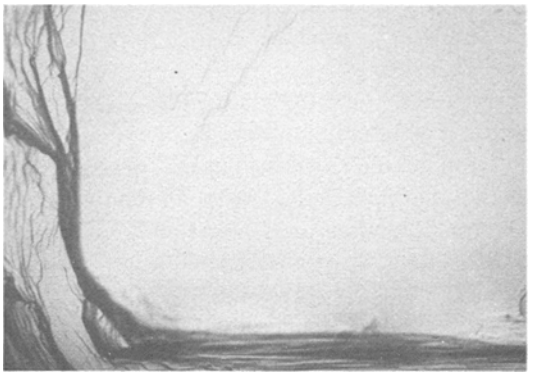

Figure 1 An as-grown (0 1 0) face supporting the layer mechanism of crystal growth (× 90).

The crystals easily cleave along (1 1 0) planes by either a sharp blade or suddenly immersing them into boiling water. A typical cleavage accompanied by the corresponding multiple beam interferogram [4] is shown in Fig. 2. Evidently, the cleavage is fairly perfect and possesses characteristics of relatively soft crystals.

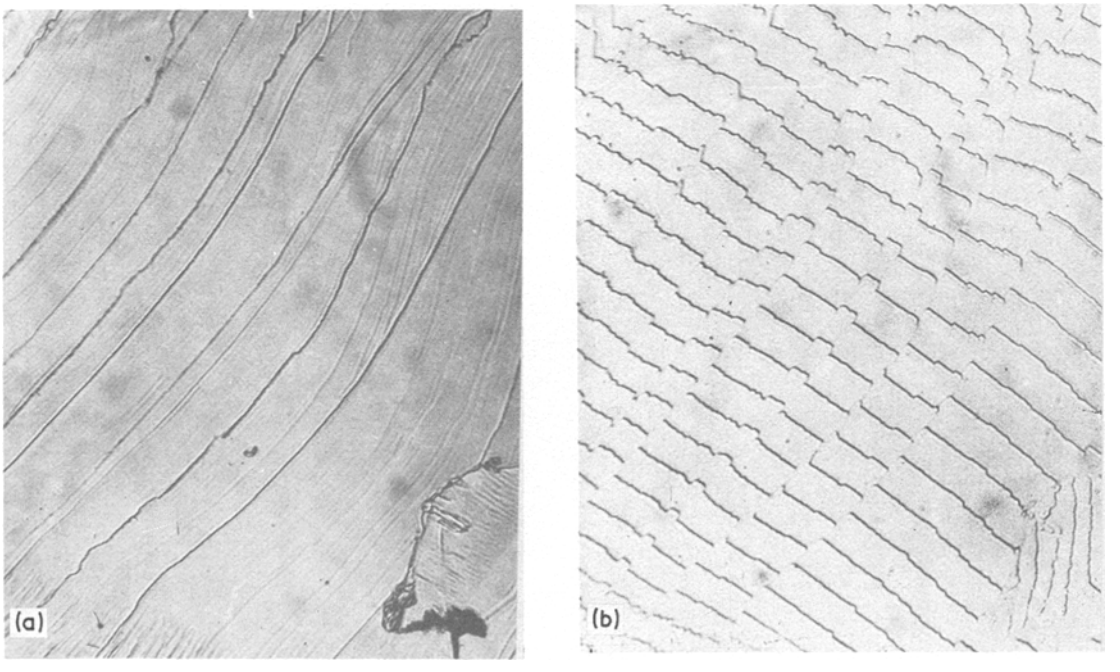

Figure 2 (a) A typical (1 1 0) cleft plane exhibiting smooth cleavage lines (× 180). (b) A multiple beam interferogram over the region of the face shown in (a) revealing the perfect nature of the crystal cleavages (× 180).

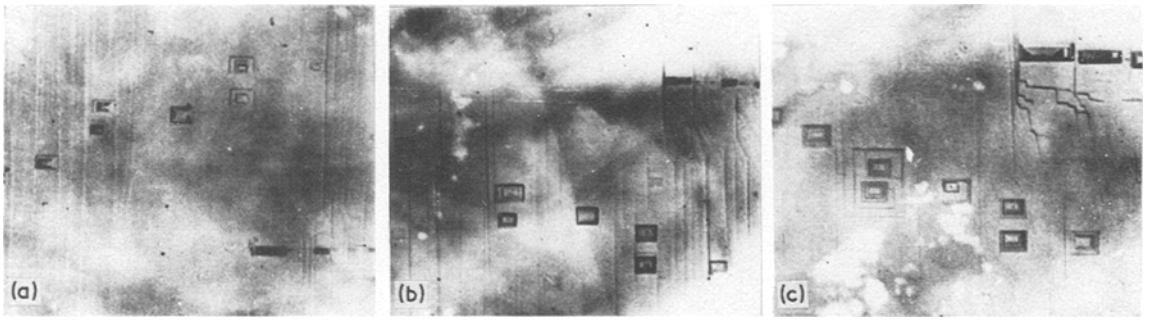

Figure 3 A demonstration of the reliability of an etchant to mark the dislocation sites. (a) A cleft face after being subjected to chemical etching; (b) a complimentary face etched for the same time as (a); and (c) the same region as (b) subjected to etching for a successive period (all × 90).

A (1 1 0) pair of cleavage faces was subjected to chemical etching for 1 min in 0.1 M NH_4Cl solution at 38° C. A typical etch pattern is shown in Figs. 3a and b. Prolonged etching of the face of Fig. 3b resulted in the pattern shown in Fig. 3c. The one-to-one correspondence of etch pits in Figs. 3a and b and no change in their number and those in Figs. 3b and c, their number and position being unchanged, is sufficient [5] to show that the above solution etches off the dislocations intersecting with (1 1 0) faces.

The rate of etching depends on several factors such as purity of the crystal, temperature of etching, stirring rate, concentration and type of the etching solution. In particular, keeping the other parameters fixed, we studied the difference in etching with aqueous NH_4Cl solution when pure, and when an additive, C_2H_5OH, was incorporated. The lateral area A of rectangular etch pits, determined to within an accuracy of 2%, is plotted in Fig. 4 as a function of time. It is noteworthy that, except in the initial stage below points A and B on the two curves, the pits expand linearly with time. From the computed etch rates, $\partial A/\partial t$, of the two solutions, see Table I, one infers that the contamination of NH_4Cl solution with C_2H_5OH probably retards the tangential etch fronts, and thus lowers the etch rate. This situation is similar to that encountered with NaCl [6, 7], where the solubility of the crystal is increased by the addition of water to ethanol and acetic acid.

When (1 1 0) planes of rectangular needles [2], grown along [0 0 1], were etched (Fig. 5), the dislocation density was found to be more in the middle region than that near the edges. This observation is contradictory to the general view of a larger dislocation density near the edges [8] and needs explanation. The freely suspended needle

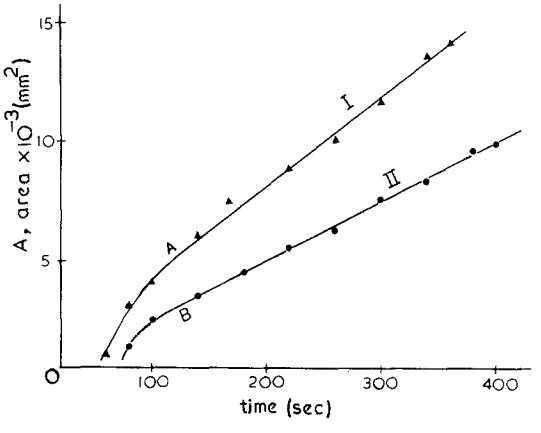

Figure 4 Graphical analysis of the variation in pit dimension, A, (measured by the expansion of the lateral area of etch pits) with the time of etching using aqueous NH_4Cl (curve I) and aqueous $NH_4Cl + C_2H_5OH$ (curve II).

TABLE I

Etching agent	Temperature of etching (° C)	Representative curve	Etch rate, $\partial A/\partial t$ ($mm^2\ sec^{-1}$)
0.1 M NH_4Cl solution in distilled water	38	I	3.9×10^{-5}
20 ml above etchant plus 5 ml C_2H_5OH	38	II	2.3×10^{-5}

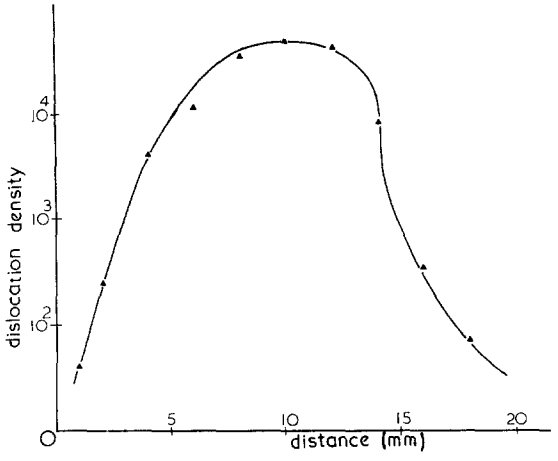

Figure 5 Graphical representation of the change in dislocation density along the length of a typical [0 0 1] needle. Evidently, the grown-in dislocations are more concentrated in the middle portion of the needle.

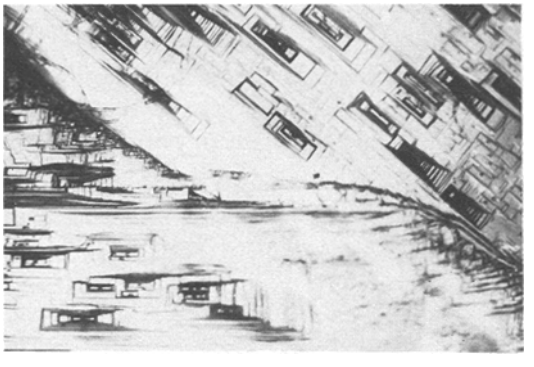

Figure 6 A typical observation illustrating the presence of twin-boundary within the crystal. On both sides of the boundary, the etch pits reveal the symmetry of the host face (× 180).

develops as a result of the growth (on an initial nucleus) from the centre outwards on both the sides. Initially the growth is expected to be rapid, because the reacting solutions have high concentrations and therefore the rates of their diffusion are likely to be large. The resulting large differentials in concentration would give rise to wide fluctuations in growth condition, and consequently, to a large number of dislocations initially. As the growth proceeds, the concentration of the reactants reduces and so does the porosity of the gel, because its cells become increasingly clogged with the waste product of the chemical reaction. This results in a decrease in diffusion rate. One would therefore expect a fewer number of dislocations in the later stages of growth, that is, near the outer edges of the crystal, as observed.

Etching has not only revealed the dislocation structure, but also a twin-boundary [9]. This is shown in Fig. 6. The angle of orientation between the pits on the two sides of the boundary is nearly 39° which indicates that it must have been formed due to a junction of (1 0 0) with (1 1 0).

On some of the cleavages, tilt-boundaries were revealed by etching, as illustrated in Fig. 7a. Refocusing below the cleavage surface exhibited the pattern shown in Fig. 7b. This suggests that inclusions tend to segregate preferentially along grain boundaries. That the generation of the tilt boundary is not a consequence of the precipitation of inclusions is obvious from the observation that at other sites (say, region around A containing randomly distributed inclusions) on the face the etch pits are not found associated with inclusions.

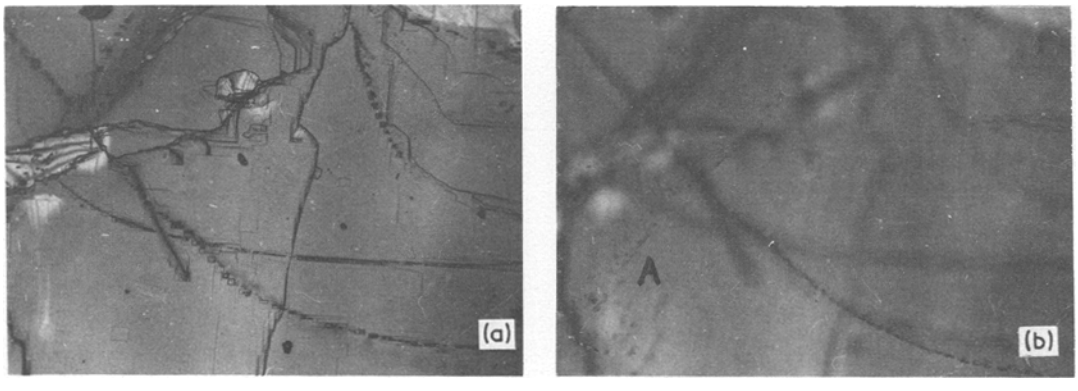

Figure 7 (a) Chemical etching of a cleavage face reveals the presence of a typical row of pits resembling a low-angle grain boundary (× 70). (b) the same face, when focussed slightly below the surface, shows the presence of a row of inclusions. Region marked A represents a random colony of inclusions (× 70).

This contradicts the general observation of dislocation nucleation at a chemical stress concentration [10–12].

The formation of these inclusions probably involves the trapping of either the reactant or the waste product, possibly interstitially, followed by its migration to dislocations, or even directly along dislocation lines [13]. Agglomeration of the trapped liquid could then occur by a mechanism similar to the one proposed by Amelinckx *et al.* [14].

The Vickers microhardness of the crystals [15] was computed using the formula VHN = 1.8547 P/d^2 g mm^{-2}. The measurements of diagonals were made at 23° C, 41% r.h.

Experiments were first performed to ascertain whether the microhardness varied with loading time. For the purpose, a pair of mirror cleavages was selected. One face was kept immersed in distilled water for 2 days (wet condition) while its counterpart was placed for 2 days in a closed vessel containing phosphorus penta-oxide (dry condition). The results of static indentation using a load of 20 g on the two halves are represented graphically in Fig. 8. It is implied that VHN is necessarily a function of the duration of indentation. Moreover, while VHN of the sample under dry weather is constant, that under humid weather falls. The slow decrease in VHN is due to a finite time required for HOH molecules to reach and lubricate the newly created indentor–specimen interface. It appears that OH^- ions probably play a vital role in the water-induced softening mechanism [16, 17] which operates to relax the local distortion in the lattice.

VHN was determined as a function of indentor load, and the results are shown graphically in Fig. 9. They reveal that VHN rises monotonically with load before attaining a maximum value of 88.6 at about 90 g. So, for loads below 90 g, VHN is load-dependent. This may be explained in terms of the effect of distorted zone of the crystal, as suggested by Berzina *et al.* [18]. During the process of indentation, the indentor penetrates a depth comparable with, or greater than, the thickness of the distorted zone. Since this zone is pierced by the indentor, its effects will be marked at relatively low loads, and hence we observe a steady increase in the hardness with load. For

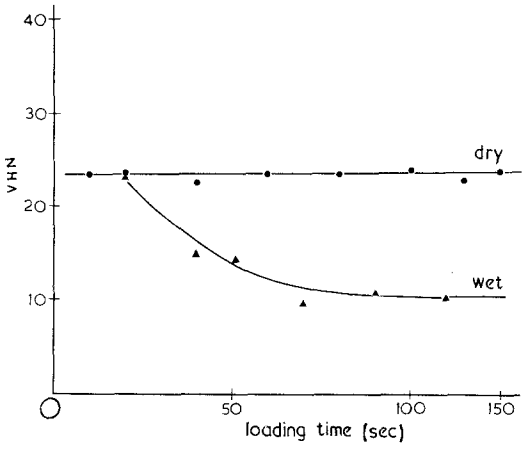

Figure 8 A graph showing the influence of the external environment of the sample on the change in microhardness with time.

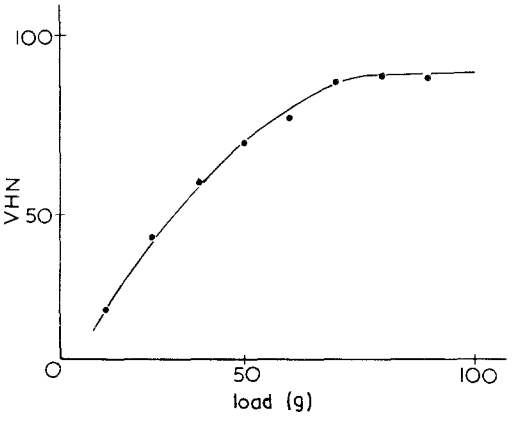

Figure 9 A plot showing variation of the Vickers microhardness of the crystal with applied load.

larger loads (greater than 90 g), the indentor might be reaching a depth at which undistorted layers of material exist and the microhardness ceases to depend on load.

The breaking strength in compression of the crystals of SrTr was measured using an Instron Universal Tensile Testing machine at 26° C and 48% r.h. The cross-head speed employed was 5 mm sec^{-1}. Compressions were applied in two different directions; parallel planes of a prism and basal pinacoid habit [2] of the virgin specimens resulted a strength of 6.763×10^6 g cm^{-2}, whereas that between (0 0 1) planes was 1.102×10^5 g cm^{-2}. It is evident that much less energy is required to

break the covalent bonding perpendicular to (0 0 1) plane. This undoubtedly supports the existence of an easy (1 1 0) cleavage in these crystals. It may be mentioned that along both the directions the strain varied linearly with stress before the crystals broke under compression.

When an indented face was subjected to etching, considerable random cracking was observed around the indentation mark, and no rosette pattern was formed, indicating that the crystals do not undergo plastic deformation at room temperature. This view is also supported by our hardness experiments. High temperature might produce slip. The density of transparent crystals, determined by the bottle method [19] at 28° C, was 2.003 g ml^{-1}. The solubility in water was found, using stoppered flasks, to be 0.0689 g per 100 ml at 28° C. The specific resistivity at 26° C was observed to be 5.3×10^9 Ω cm.

Acknowledgements

Many thanks are extended to Dr K. Sangwal for useful discussions and help in writing the manuscript, and to Dr C. K. Patel for the help rendered in using Instron Machine.

References

1. H. K. HENISCH, J. DENNIS and J. I. HANOKA, *J. Phys. Chem. Solids* **26** (1965) 493.
2. A. R. PATEL and S. K. ARORA, *J. Mater. Sci.* **11** (1976) 843.
3. R. F. STRICKLAND-CONSTABLE, "Kinetics and Mechanism of Crystallization" (Academic Press, London, 1968) p.1.
4. S. TOLANSKY, "Multiple Beam Interferometry" (Oxford University Press, Oxford, 1947).
5. W. G. JOHNSTON, "Progress in Ceramic Science", Vol. 2. edited by J. E. Burke (Pergamon Press, New York, 1962).
6. V. N. ROCHANSKII, E. V. PARVOVA, V. M. STEPANOVA and A. R. PREDVODITELEV, *Sov. Phys. Crystal.* **6** (1962) 564.
7. N. F. KOSTIN, S. V. LUBENETS and K. S. ALEKSANDROV, *ibid* **6** (1962) 588.
8. KH. S. BAGDASAROV, E. R. DOBROVINSKAYA, V. V. PISHCHIK, M. M. CHERNIK, YU. YU. KOVALOV, A. S. GERSHUN and I. F. ZVYAGINTSEVA, *ibid* **18** (1973) 242.
9. M. J. BUERGER, *Amer. Mineral.* **30** (1945) 469.
10. A. S. PARASNIS and J. W. MITCHEL, *Phil. Mag.* **4** (1959) 171.
11. M. S. JOSHI and B. K. PAUL, *J. Crystal Growth* **22** (1974) 326.
12. A. R. PATEL and S. K. ARORA, *ibid* **23** (1974) 95.
13. K. A. GROSS, *ibid* **6** (1970) 210.
14. S. AMELINCKX, W. MAENHOUT-VAN DER VORST and W. DEKEYSER, *Acta Met.* **7** (1959) 8.
15. B. W. MOTT, "Microindentation Hardness Testing" (Butterworth, London, 1956).
16. J. H. WESTBROOK, "Environment Sensitive Mechanical Behaviour", edited by A. R. L. Westbrook and N. S. Stoloff, (Gordon–Breach, New York, 1967).
17. R. E. HANNEMAN and J. H. WESTBROOK, *Phil. Mag.* **18** (1968) 73.
18. I. G. BERZINA, I. B. BERMAN and P. A. SAVINTSEV, *Sov. Phys. Cryst.* **9** (1965) 483.
19. A. FINDLAY, "Practical Physical Chemistry", 8th edition, (Longmares Green, London, 1954).

Received 9 November 1976
and accepted 9 March 1977

A. R. PATEL
S. K. ARORA
Department of Physics,
Sardar Patel University,
Vallabh Vidyanagar 388120,
Gujarat State, India

On the spark machining of cubic Laves-phase compounds which contain gadolinium

The cubic Laves-phase compounds of gadolinium are of interest to research workers in the fields of Mössbauer spectroscopy and nuclear magnetic resonance because the nature of the hyperfine field at the lattice sites yields information on the nature of the spin-exchange interactions in the bulk material. The gadolinium compounds which are, at present, of most interest are $GdFe_2$ and $GdCo_2$. These compounds are manufactured by melting a stoichiometric mixture of gadolinium and iron or cobalt powders in either an electron beam furnace or an argon arc furnace. Once the molten state has been reached the samples are quenched rapidly to room temperature. They are then turned over and the samples remelted. This procedure is performed several times to ensure homogeneity within the sample. Ingot sizes are usually small: typically they are produced as cylinders having diameters of about 10 mm and heights of about 4 mm.

After the ingots of the compounds have been manufactured they have to be converted into the